
FRAug: Tackling Federated Learning with Non-IID Features via Representation Augmentation

Haokun Chen^{1,2} * Ahmed Frikha^{1,2} Denis Krompaß¹ Volker Tresp^{1,2}

¹Siemens Technology, Munich, Germany

²Ludwig Maximilian University of Munich, Germany

Abstract

Federated Learning (FL) is a decentralized learning paradigm in which multiple clients collaboratively train deep learning models without centralizing their local data and hence preserve data privacy. Real-world applications usually involve a distribution shift across the datasets of the different clients, which hurts the generalization ability of the clients to unseen samples from their respective data distributions. In this work, we address the recently proposed feature shift problem where the clients have different feature distributions while the label distribution is the same. We propose Federated Representation Augmentation (FRAug) to tackle this practical and challenging problem. Our approach generates synthetic client-specific samples in the embedding space to augment the usually small client datasets. For that, we train a shared generative model to fuse the clients' knowledge, learned from different feature distributions, to synthesize client-agnostic embeddings, which are then locally transformed into client-specific embeddings by Representation Transformation Networks (RTNets). By transferring knowledge across the clients, the generated embeddings act as a regularizer for the client models and reduce overfitting to the local original datasets, hence improving generalization. Our empirical evaluation on multiple benchmark datasets demonstrates the effectiveness of the proposed method, which substantially outperforms the current state-of-the-art FL methods for non-IID features, including PartialFed and FedBN.

1 Introduction

Federated Learning (FL) is a machine learning paradigm in which a shared model is collaboratively trained using decentralized data sources. In the classic FL, i.e., FedAvg [33], the central server obtains the model by iteratively aggregating and averaging the optimized parameters from the active clients, which does not require direct access to the clients' local data and therefore preserves the data confidentiality.

However, traditional FL suffers from performance degradation when the data is heterogeneous across the clients [44]. Several methods [26, 37] were developed to tackle problem settings where the clients have different label distributions. We focus on the recently proposed [28] underexplored problem of heterogeneity in the feature space, i.e., the distributions of the input features from different clients are not identical, hence the overall data is non-IID. This problem setting is of great practical value since it is present in multiple real-world scenarios where different entities have local data following different feature distributions. For instance, in the healthcare sector, different clinical centers use different scanners and data acquisition protocols, resulting in a distribution shift in the input space

* Correspondence to: haokun.chen@siemens.com

of the collected medical images [7]. Analogously, in industrial manufacturing, the data collected by machines from different manufacturers, possibly using different sensors, in different production plants, exhibit feature distribution shift. Most importantly, although these commercial entities have the same application, e.g., diagnosing the same type of cancer or detecting the same types of anomalies, they may not be willing to share their original data to prevent competitive disadvantage. Therefore, FL for non-IID features provides the benefit of training a machine learning model collaboratively in a decentralized, data-privacy-preserving manner.

In this paper, we propose Federated Representation Augmentation (FRAug) to address the feature shift problem in FL. In FRAug, we first aggregate the knowledge of different clients in the feature space by learning a shared generator, which is optimized to produce client-agnostic feature embeddings. Then, a Representation Transformation Network (RTNet) is locally trained for each client, which transforms the client-agnostic representations into client-specific representations. Finally, we use both the client local dataset, as well as the client-specific synthetic embeddings to obtain the classification model with better generalization ability. We demonstrate the effectiveness of FRAug by empirically evaluating it on real-world FL benchmarks with non-IID features, where our method outperforms the classic FL baselines FedAvg [33], as well as the recently proposed methods for FL with feature shift.

2 Related Work

Federated Learning (FL): Federated Averaging (FedAvg) [33] is one of the classic FL algorithms for training machine learning models using decentralized data sources. This simple paradigm suffers from performance degradation when there exists data heterogeneity [20, 25]. Numerous studies have been conducted for label space heterogeneity, i.e., class distributions are imbalanced across different clients, by regularizing local update with proximal term [26], personalizing client models [2, 8, 37, 27], utilizing shared local data [44, 30, 10], introducing additional proxy datasets [24, 29, 11], or performing data-free knowledge distillation [32] in the input space [13, 42, 43] or the feature space [15, 48]. However, there are only limited studies addressing the heterogeneity in feature space, i.e., non-IID features. Recently, [1] showed that Batch Normalization layers (BN) [18] with local-statistics improve the robustness of the FL model to inter-center data variability and yield better out-of-domain generalization results, while FedBN [28] provided more theoretical analysis on the benefits of local BN layers for FL with feature shift. PartialFed [36] empirically found that partially initializing the client models could alleviate the effect of feature distribution shift. In this work, we tackle the problem of non-IID features in FL via a client-specific data augmentation approach performed in the embedding space. In particular, client-agnostic embeddings are initially synthesized by a shared generator that captures the knowledge from different distributions, which are then personalized by separate client-specific models. Training the local models with the resulting client-specific embeddings yields a higher generalization to unseen data from the local distribution.

Cross-Domain Learning: The problem of learning on centralized data with non-IID features, i.e., cross-domain data, has been widely studied in the context of Unsupervised Domain Adaptation (UDA) [39], where a model is trained using multiple source domains and finetuned using an unlabelled target domain, and Domain Generalization (DG) [46], where the target domain data is not accessible during the training process of UDA. A variety of efforts have been made to tackle the problem of UDA and DG. CROSSGRAD [35] used adversarial gradients obtained from a domain classifier to augment the training data. L2A-OT [45] trained a generative model to transfer the training samples into pseudo novel domains. MixStyle [47] performed feature-level augmentation by interpolating the style statistics of the output features from different network layers. While the aforementioned methods assume centralized access to all datasets from different domains, we address the problem where the datasets are decentralized and cannot be shared due to privacy concerns.

3 Methodology

3.1 Problem Statement: Federated Learning (FL) with Non-IID Features

In this work, we address an FL problem setting with non-IID features, which we describe in the following. Let $\mathcal{X} \subset \mathbb{R}^{d_{in}}$ be an input space, $\mathcal{U} \subset \mathbb{R}^{d_u}$ be a feature space, and $\mathcal{Y} \subset \mathbb{R}$ be an output space. Let $\theta := [\theta_f, \theta_h]$ denote the parameters of the classification model trained in an FL setting involving one central server and $K \in \mathbb{N}$ clients. The model consists of two components: a feature

extractor $f : \mathcal{X} \rightarrow \mathcal{U}$ parameterized by θ_f , and a prediction head $h : \mathcal{U} \rightarrow \mathcal{Y}$ parameterized by θ_h . We assume that a dataset $D^k = \{(\mathbf{x}_i^k, y_i^k) | i \in \{1, \dots, N_k\}\}$, containing private data, is available on each client, where $N^k \in \mathbb{N}$ denotes the number of samples in D^k and $C \in \mathbb{N}$ denotes the number of classes. As discussed in [20], FL with non-IID data can be described by the distribution shift on local datasets: $P_{\mathcal{X}\mathcal{Y}}^{k_1} \neq P_{\mathcal{X}\mathcal{Y}}^{k_2}$ with $\forall k_1, k_2 \in \{1, \dots, K\}, k_1 \neq k_2$, where $P_{\mathcal{X}\mathcal{Y}}^k$ defines the joint distribution of input space \mathcal{X} and label space \mathcal{Y} on D^k . The addressed problem setting, i.e., FL with non-IID features, covers (1) *covariate shift*: The marginal distribution $P_{\mathcal{X}}$ varies across clients, while $P_{\mathcal{Y}|\mathcal{X}}$ is the same, and (2) *concept shift*: The conditional distribution $P_{\mathcal{X}|\mathcal{Y}}$ varies across clients, while $P_{\mathcal{Y}}$ is the same [28]. From the perspective of cross-domain learning [39, 46] literature, local data from every client can be viewed as a separate domain. In this work, we use *cross-domain FL* and *FL with non-IID features* interchangeably.

3.2 Motivational Case Study

To motivate our representation augmentation algorithm, we present an empirical analysis to address the following research question: In a data scarce scenario, does finetuning only the prediction head using additional feature embeddings leads to performance improvement? For this, we conduct local training experiments on each client, i.e., without federated learning. First, we optimize a classification model θ^k with 10% of the local dataset D^k . As a result, each client has ca. 100 to 1000 data samples available for training, which matches the experimental settings used in prior FL work [33, 28]. Then, we fix the parameters of the feature extractor f , i.e., θ_f^k , and finetune *only* the prediction head with 100% of D^k . Finally, we evaluate both classification models, i.e., the model fully trained with 10% of the data, and its finetuned version where the prediction head is further trained with embeddings of 100% of the examples. We note that both models use the same feature extractor that was trained with 10% of the data.

Method	OfficeHome					PACS				
	A	C	P	R	Avg	A	C	P	S	Avg
w/o finetune	35.80	45.54	67.04	61.16	52.42	82.37	86.08	92.01	87.52	87.00
w. finetune	69.96	72.31	86.04	80.50	77.20	88.46	88.61	97.08	92.21	91.59

Table 1: Performance comparison of the classification model θ^k with (w.) and without (w/o) prediction head finetuning using embeddings of additional examples.

Table 1 shows the classification performance on the OfficeHome [38] and PACS [23] datasets, where each client holds data from one domain. We find that optimizing only the prediction head with additional embeddings, leads to an average improvement of 24.78% for OfficeHome and 4.59% for PACS, a substantial performance boost. These results show that the feature extractor, trained with less data, still captures useful information when exposed to unseen image samples and give evidence of the applicability and effectiveness of data augmentation methods in the embedding space, in scarce data settings. We leverage this observation when designing the proposed method.

3.3 FRAug: Federated Representation Augmentation

To tackle FL with non-IID features, we propose Federated Representation Augmentation (FRAug). Our algorithm is built upon FedAvg [33] which is the most widely used FL strategy. In FedAvg, the central server sends a copy of the global model θ to each client to initialize their local models $\{\theta^k | k \in K\}$. After training on its local dataset D^k , the client-specific updated models are sent back to the central server where they are averaged and used as the global model. Such communication rounds are repeated until some predefined convergence criteria are met. Similarly, the training process of FRAug (Algorithm 1) can be divided into two stages: (1) The *Server Update*, where the central server aggregates the parameters uploaded by the clients and distributes the averaged parameters to each client, and (2) the *Client Update*, where each client receives the model parameters from the central server and performs local optimization. Unlike FedAvg, where only the local dataset of each client is used for training, FRAug generates additional feature embeddings to finetune the prediction head of the local classification model. Concretely, we train a shared generator and a local Representation

Transformation Network (RTNet) for each client, which together produce *domain-specific*¹ synthetic feature embeddings for each client to augment its local data in the embedding space. Hereby, the shared generator captures knowledge from all the clients to generate client-agnostic embeddings, which are then personalized by the local RTNet into client-specific embeddings. In the following, we provide a more detailed explanation of FRAug.

3.3.1 Server Update

At the beginning of the training, the server initializes the parameters of the classification model $\theta := [\theta_f, \theta_h]$, as well as the *shared* generator ω . In each communication round r , all clients receive the aggregated model parameters and conduct the *Client Update* procedure in parallel. Subsequently, the server securely aggregates the optimized model parameters from all the clients into a single model that is used in the next communication round.

3.3.2 Client Update

An overview of the client learning procedure is illustrated in Figure 1. At the beginning of the first communication round, each client *locally* initializes a Representation Transformation Network (*RTNet*) parameterized by ϕ^k . Subsequently, each client receives the classification model parameters θ^k and the generator parameters ω^k from the server, and conducts T local update steps. Each local update comprises 2 stages: (1) Classification model optimization, and (2) Generator and RTNet optimization.

Classification Model Optimization: In this stage, the generator and the RTNet are fixed, while the classification model is updated by minimizing the loss \mathcal{L}_{cls} , where

$$\mathcal{L}_{cls} = \mathcal{L}_{real} + \mathcal{L}_{syn}. \quad (1)$$

While \mathcal{L}_{real} is minimized to update the model parameter θ^k by using real training samples from D^k , \mathcal{L}_{syn} is minimized to update only the prediction head h^k as it is computed on synthetically generated samples in the embedding space \mathcal{U} . We use cross-entropy (L_{CE}) for both loss functions.

To generate domain-specific synthetic embeddings, the shared generator g^k and local RTNet m^k are used to generate residuals that are added to the embeddings of real examples produced by the local feature extractor h^k . Hereby, we first generate client-agnostic embeddings \hat{v}^k by feeding a batch of random vector $z \sim \mathcal{N}(0, I)$ and class labels y into the generator g^k . Subsequently, \hat{v}^k are transformed by the local RTNet into client-specific residuals and added to the embeddings of real datapoints. We distinguish two types of synthetic embeddings that we generate to train the local prediction head: domain-specific synthetic embeddings \hat{u}^k and class-prototypical domain-specific synthetic embeddings \hat{u}_c^k . The domain-specific embeddings \hat{u}^k are generated by adding synthetic residuals to the embeddings u^k of real examples from the current batch sampled from D^k . On the other hand, synthetic residuals are added to class-prototypes \bar{u}_c^k , i.e., class-wise average embeddings of real examples, to produce \hat{u}_c^k .

$$\mathcal{L}_{syn} = L_{CE}(h^k(\hat{u}^k), y) + \sum_{c \in C} L_{CE}(h^k(\hat{u}_c^k), c), \quad (2)$$

$$\text{with } \hat{u}^k = u^k + \lambda_{syn} \cdot m^k(g^k(z, y)), \quad \hat{u}_c^k = \bar{u}_c^k + \lambda_{syn} \cdot m^k(g^k(z', c)). \quad (3)$$

We note that, for the generation of \hat{u}^k , the original labels y of the sampled data batch are used for the residual generation, since the residuals are added to the embeddings of the examples corresponding to these labels. For \hat{u}_c^k , we feed the label c that correspond to the class of the average embedding \bar{u}_c^k . The class-prototypical client-specific embeddings \hat{u}_c^k are generated to stabilize the training and increase the variance of the generated embeddings.

¹Since each client has data from a different domain, we use *domain-specific* and *client-specific* interchangeably.

While the residuals produced by the generator and the RTNet are random in early training iterations due to the random initialization of these models, they become more informative as training progresses. To reflect this in our algorithm, we employ the weighting coefficient λ_{syn} that controls the impact of the residuals, and increase it following an exponential schedule throughout training.

To compute the class-wise average embedding $\bar{\mathbf{u}}_c^k$, we use the exponential moving average (EMA) scheme, at each local iteration. In particular,

$$\bar{\mathbf{u}}_c^k = (1 - \lambda_c) \cdot \bar{\mathbf{u}}_c'^k + \lambda_c \cdot \frac{\sum_{i \in B} \mathbb{1}(y_i = c) \cdot f(\mathbf{x}_i)}{\sum_{i \in B} \mathbb{1}(y_i = c) + \epsilon}, \quad (4)$$

where $\mathbb{1}(\cdot)$ denotes the indicator function, B is the batch size of the real samples, $\bar{\mathbf{u}}_c'^k$ is the class-wise average embedding computed on the previous local iteration, and ϵ is a small number added for numerical stability. By using the average embeddings of previous iterations, we enable the examples of previously sampled batches to contribute to the computation of the current average embeddings. The ratio λ_c follows an exponential ramp-up schedule as proposed in [21].

To allow the different client-specific models to learn feature extractors tailored to their data distribution D^k , while still benefiting from the collaborative learning, we use local Batch Normalization layers (BN) [18] as introduced in [28].

Generator and RTNet Optimization: In the second stage, the classification model is fixed while the generator and the RTNet are optimized. The class-conditional generator g^k takes a batch of random vectors \mathbf{z} and class labels \mathbf{y} to produce *client-agnostic* feature embeddings $\hat{\mathbf{v}}^k$. $\hat{\mathbf{v}}^k$ are then fed into the RTNet m^k to be adapted to the feature distribution of the corresponding client k . The resulting residuals are added on the embeddings of real examples to produce the *domain-specific* synthetic embeddings $\hat{\mathbf{u}}^k$ and $\hat{\mathbf{u}}_c^k$. The generator will be optimized by minimizing the loss \mathcal{L}_{gen} , with

$$\mathcal{L}_{gen} = L_{CE}(h(\hat{\mathbf{u}}^k), y) - \alpha L_{MMD}(\hat{\mathbf{u}}^k, \mathbf{u}^k). \quad (5)$$

The minimization of the cross-entropy loss L_{CE} incentivizes the shared generator to produce features that are recognized by the prediction heads of all the clients. By sharing and optimizing the generator across all clients, we ensure that the synthetic embeddings produced by the generator, i.e., $\hat{\mathbf{v}}^k$, capture client-agnostic semantic information. Additionally, we maximize the statistical distance [40] between $\hat{\mathbf{u}}^k$ and the real feature embeddings \mathbf{u}^k . By doing so, we force $\hat{\mathbf{v}}^k$ not to follow any client-specific distribution, and thus enhance the variance of the augmented feature space. Here, we adopt Maximum Mean Discrepancy (MMD) [12] as the distance metric. Subsequently, the client-agnostic embeddings are fed into the RTNet m^k parametrized by ϕ^k to produce domain-specific embeddings $\hat{\mathbf{u}}^k$ and $\hat{\mathbf{u}}_c^k$. ϕ^k is optimized by minimizing the loss \mathcal{L}_{rt} , where

$$\begin{aligned} \mathcal{L}_{rt} = & - (L_{ent}(h(\hat{\mathbf{u}}^k)) + \sum_{c \in C} L_{ent}(h(\hat{\mathbf{u}}_c^k))) \\ & + \beta (L_{MMD}(\hat{\mathbf{u}}^k, \mathbf{u}^k) + \sum_{c \in C} L_{MMD}(\hat{\mathbf{u}}_c^k, \bar{\mathbf{u}}_c^k)). \end{aligned} \quad (6)$$

Here, we maximize the entropy (L_{ent}) of the prediction head output on $\hat{\mathbf{u}}^k, \hat{\mathbf{u}}_c^k$ to incentivize the generation of synthetic embeddings that are *hard* to classify for the prediction head h . To avoid generating outliers, we add a regularization term that minimizes the Maximum Mean Discrepancy (MMD) between real and synthetic embeddings. In particular, we penalize high MMD distances between $\hat{\mathbf{u}}^k$ and $\hat{\mathbf{u}}^k$, as well as $\hat{\mathbf{u}}_c^k$ and $\bar{\mathbf{u}}_c^k$, for each class c . α and β denote weighting coefficients in Eq. 5 and 6, respectively.

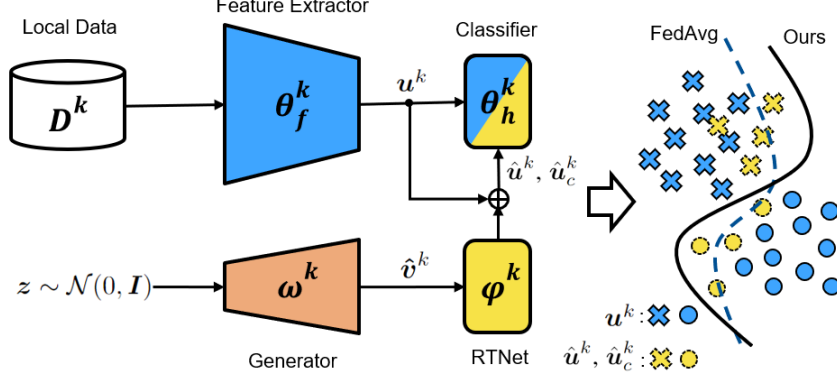


Figure 1: Overview of FRAug local update at client k : a shared generator is learned to aggregate knowledge from multiple clients and generate client-agnostic feature embeddings \hat{v}^k , which are then fed into the local Representation Transformation Network ($RTNet$) to produce domain-specific feature embeddings \hat{u}^k and \hat{u}_c^k . Finally, the real feature embeddings u^k , extracted by the feature extractor using local dataset D^k , will be augmented with \hat{u}^k and \hat{u}_c^k in the prediction head optimization, which leads to a classification model with better generalization ability.

Algorithm 1: Training procedure of Federated Representation Augmentation (FRAug)

```

1 ServerUpdate
2   Randomly initialize  $\theta_0, \omega_0$ 
3   for round  $r \leftarrow 1$  to  $R$  do
4     for client  $k \leftarrow 1$  to  $K$  in parallel do
5        $\theta_r^k, \omega_r^k \leftarrow$  ClientUpdate  $(\theta_{r-1}, \omega_{r-1}, k, r)$ 
6     end
7      $\theta_r \leftarrow \frac{1}{K} \sum_{k=1}^K \theta_r^k$ 
8      $\omega_r \leftarrow \frac{1}{K} \sum_{k=1}^K \omega_r^k$ 
9   end
10
11 ClientUpdate( $\theta, \omega, k, r$ )
12   if  $r = 1$  then
13     Randomly initialize  $\phi^k$ 
14   end
15    $\theta^k \leftarrow \theta, \omega^k \leftarrow \omega$ 
16   for local training iteration  $t \leftarrow 1$  to  $T$  do
17     Sample  $\{\mathbf{X}, \mathbf{y}\}$  from  $D_k$ 
18     Sample  $\mathbf{z}, \mathbf{z}' \sim \mathcal{N}(0, I)$ 
19     Fix  $\phi^k$  and  $\omega^k$ , and optimize  $\theta^k$  using Equation 1
20     Fix  $\theta^k$ , and optimize  $\phi^k$  and  $\omega^k$  using Equation 5 and 6, respectively
21   end
22   return  $\theta^k, \omega^k$ 

```

4 Experimental Results

4.1 Dataset Description

We perform an extensive empirical analysis² using three real-world image classification datasets with domain shift: (1) *OfficeHome* [38], which contains 65 classes in four domains: Art (A), Clipart (C), Product (P) and Real-World (R). (2) *PACS* [23], which includes images that belong to 7 classes from four domains Art-Painting (A), Cartoon (C), Photo (P) and Sketch (S). (3) *Digits* comprises images

²Code will be made public upon paper acceptance.

of 10 digits from the following four datasets: MNIST (MT) [22], MNIST-M (MM) [9], SVHN (SV) [34] and USPS (UP) [17]. Each client contains data from one of the domains, i.e., there exists feature shift across different clients. To simulate data scarcity described in Section 3.2, we assume that only 10% (1% for the Digits dataset) of the original data is available for each client, resulting in ca. 100 to 1000 data samples per client following the experimental setup in the previous work [33, 28].

4.2 Implementation Details

For the OfficeHome and PACS datasets, we use a ResNet18 [16] pretrained on ImageNet [5] as initialization of the classification model. For Digits, we use a 6-layer Convolution Neural Network (CNN) as the backbone. We adopt a 2-layer MLP as the generator and RTNet architectures for all datasets. In the appendix, we provide further details about model architectures and training hyperparameters. All experiments are repeated with 3 different random seeds.

4.3 Results and Discussion

We compare our approach with several baseline methods, including *Single*, i.e., training an individual model on each client separately, *All*, i.e., training a single model at the central server using data aggregated from all clients, *FedAvg* [33], *pFedAvg*, i.e., FedAvg with local model personalization, and *FedProx* [26]. We note that *All* is an oracle baseline as it requires centralizing the data from the different clients, hence infringing the data-privacy requirements. Furthermore, we compare our method with the current state-of-the-art FL methods for non-IID features, i.e., *FedBN* [28] and *PartialFed* [36]. We use the published code of *FedBN* and reimplement *PartialFed* since the original implementation was not made public. We conduct the same hyperparameter search for all methods and report the best results. Detailed hyperparameter search space of different methods are provided in the Appendix.

We report the accuracies achieved by the different methods on all three datasets in Table 2. We observe that FRAug outperforms all the baselines on all benchmark datasets. On OfficeHome, FRAug outperforms FedAvg and FedBN by 1.91% and 1.58%, respectively. On Digits, FRAug achieves a substantial 2.3% improvement on average compared with all the alternative methods. Likewise, FRAug yields the highest average accuracy on PACS. We find that the performance improvement compared to the best baseline is the highest on the most challenging domains, i.e., on which all methods yield lower results than on other domains. These include MNIST-M and SVHN from Digits, as well as Clipart from OfficeHome, where FRAug achieves impressive improvements of above 3%. Interestingly, our approach outperforms the centralized baseline *All*, demonstrating the effectiveness of the generated embeddings in aggregating the knowledge from different clients to enable a client-specific augmentation.

Table 2: Accuracy results on different benchmark datasets with feature shift.

Benchmark	Single	All	FedAvg	FedProx	pFedAvg	PartialFed	FedBN	FRAug	
OfficeHome	A	35.80 \pm 0.1	56.65 \pm 0.7	57.47 \pm 0.6	55.68 \pm 0.4	52.50 \pm 0.9	48.83 \pm 0.2	57.59 \pm 0.8	57.61 \pm 0.6
	C	45.54 \pm 0.8	58.81 \pm 1.6	56.74 \pm 0.9	56.88 \pm 0.5	52.09 \pm 1.1	49.96 \pm 0.2	56.52 \pm 0.3	60.03 \pm 0.5
	P	67.04 \pm 0.8	71.39 \pm 0.3	73.32 \pm 0.8	73.84 \pm 0.3	71.78 \pm 0.8	72.22 \pm 0.8	73.55 \pm 1.0	74.03 \pm 0.8
	R	61.16 \pm 0.7	72.63 \pm 1.3	71.25 \pm 0.3	72.15 \pm 0.9	66.28 \pm 0.4	65.82 \pm 0.6	72.40 \pm 0.9	74.58 \pm 0.4
	avg	52.42 \pm 0.4	64.87 \pm 0.9	64.69 \pm 0.6	64.63 \pm 0.6	60.67 \pm 0.7	59.20 \pm 0.5	65.02 \pm 0.7	66.60 \pm 0.3
Digits	MT	96.68 \pm 0.2	97.04 \pm 0.1	96.85 \pm 0.1	96.90 \pm 0.1	96.40 \pm 0.2	97.13 \pm 0.1	97.03 \pm 0.1	97.81 \pm 0.1
	MM	77.77 \pm 0.5	77.04 \pm 0.1	73.51 \pm 0.2	72.60 \pm 0.4	77.56 \pm 0.4	74.21 \pm 0.5	77.02 \pm 0.2	81.65 \pm 0.5
	SV	75.55 \pm 0.3	77.96 \pm 0.5	74.49 \pm 0.2	73.01 \pm 0.5	77.50 \pm 0.1	78.10 \pm 0.5	77.59 \pm 0.1	81.24 \pm 0.3
	UP	79.93 \pm 0.8	97.13 \pm 0.1	97.62 \pm 0.1	97.31 \pm 0.3	96.67 \pm 0.1	94.78 \pm 0.5	96.80 \pm 0.2	97.67 \pm 0.3
	avg	82.54 \pm 0.1	87.29 \pm 0.2	85.62 \pm 0.2	84.96 \pm 0.3	87.03 \pm 0.2	86.05 \pm 0.3	87.11 \pm 0.2	89.59 \pm 0.4
PACS	A	82.37 \pm 0.6	83.17 \pm 0.2	82.72 \pm 0.4	80.17 \pm 0.4	88.05 \pm 0.8	84.85 \pm 0.2	86.60 \pm 0.5	87.34 \pm 0.5
	C	86.08 \pm 0.9	86.92 \pm 0.8	84.04 \pm 1.3	82.04 \pm 0.8	86.20 \pm 0.7	87.92 \pm 0.5	87.76 \pm 1.0	88.47 \pm 0.9
	P	92.01 \pm 1.1	95.95 \pm 0.8	96.05 \pm 0.5	96.74 \pm 1.0	97.89 \pm 0.5	98.24 \pm 0.4	97.95 \pm 0.4	98.64 \pm 0.6
	S	87.52 \pm 0.8	88.70 \pm 0.7	89.50 \pm 0.7	88.50 \pm 1.0	88.89 \pm 0.9	90.10 \pm 0.8	90.75 \pm 0.3	90.95 \pm 0.4
	avg	87.00 \pm 0.5	88.68 \pm 0.6	88.08 \pm 0.9	86.86 \pm 0.9	90.26 \pm 0.6	90.28 \pm 0.7	90.76 \pm 0.3	91.34 \pm 0.1

4.4 Ablation Study

To illustrate the importance of different FRAug components, we conducted an ablation study on the OfficeHome dataset. The results are shown in Table 3. We observe that using the client-agnostic synthetic embeddings \hat{v}^k instead of the personalized versions leads to performance deterioration. This highlights the importance of the transformation into personalized client-specific embeddings. Moreover, the results reveal that both types of synthetic embeddings, i.e., \hat{u}_c^k and \hat{u}^k , yield a performance boost when used separately. Employing them together further improves the results, which demonstrates their complementarity. Finally, we find that increasing the impact of the generated residuals via the smoothing term λ_{syn} throughout training, i.e., as the generator and the RTNets continue improving, is beneficial for the overall performance. We conducted the same ablation study on the PACS and Digits datasets and observed consistent result patterns. We provide these results in the Appendix.

Table 3: Ablation study for different components of FRAug.

Generator (\hat{v})	RTNet (\hat{u})	EMA (\hat{u}_c)	Smoothing (λ_{syn})	OfficeHome				
				A	C	P	R	avg
✓				56.24 \pm 0.5	59.65 \pm 0.3	72.90 \pm 0.3	73.09 \pm 0.5	65.47 \pm 0.8
✓	✓			56.75 \pm 0.8	58.95 \pm 0.8	72.88 \pm 0.2	73.93 \pm 0.3	65.63 \pm 0.8
✓	✓		✓	57.34 \pm 0.9	59.10 \pm 0.4	73.65 \pm 0.7	74.25 \pm 0.9	66.09 \pm 0.2
✓		✓		56.93 \pm 0.9	58.50 \pm 0.8	73.35 \pm 0.9	74.39 \pm 0.4	65.79 \pm 0.9
✓	✓	✓	✓	56.65 \pm 0.2	59.50 \pm 0.7	73.50 \pm 0.5	74.31 \pm 0.9	65.99 \pm 0.3
✓	✓	✓	✓	58.16 \pm 0.8	57.89 \pm 0.3	73.12 \pm 0.3	74.15 \pm 0.6	65.83 \pm 0.3
✓	✓	✓	✓	57.61 \pm 0.9	60.03 \pm 0.8	74.03 \pm 0.3	74.69 \pm 0.2	66.60 \pm 0.4

4.5 Analysis of Local Dataset Size

We investigate the effectiveness of our personalized representation augmentation technique for different sizes of client-specific local datasets. Hereby, we vary the number of datapoints available on each client from 100% to 10% of its original local dataset. Figure 2 depicts the results of this experiment. We compare FRAug with two baseline methods on OfficeHome, and conduct the experiment with 3 different seeds. We note that FRAug consistently outperforms the baselines across all dataset sizes, except one (Clipart, 100%). Compared to FedAvg, the improvement achieved by FRAug is stable across different dataset sizes, highlighting the suitability of representation augmentation for scenarios involving non-IID features with scarce and large amounts of data. Compared to local training (*Single*) without collaboration, we observe that the performance improvement yielded by federated learning methods increases as the dataset size decreases.

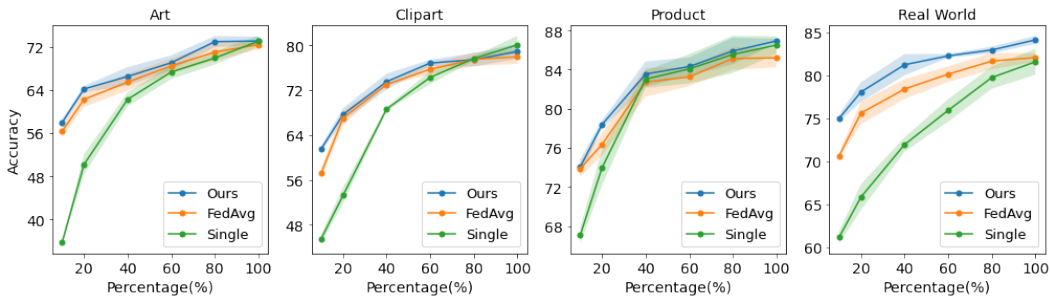


Figure 2: Performance analysis of FRAug with different local dataset sizes on client.

5 Conclusion and Outlook

In this work, we present a novel approach to tackle the underexplored feature shift problem in the federated learning (FL) setting, where the datasets of the different clients have non-IID features. Our

method, Federated Representation Augmentation (FRAug), performs client-personalized augmentation in the embedding space to improve the generalization ability of the client-specific models without sharing data in the input space. For that, we optimize a shared generative model to merge the clients’ knowledge, learned from their different feature distributions, to synthesize client-agnostic embeddings, which are then transformed into client-specific embeddings by local Representation Transformation Networks (RTNets). Our empirical evaluation on three benchmark datasets involving feature distribution shift demonstrated the effectiveness of our method which outperformed the prior approaches, achieving new state-of-the-art results in this underexplored FL setting.

While our empirical evaluation focused on image datasets, it would be interesting to apply FRAug to other data types, such as time-series data [31] or textual data [14], since it is data-type-agnostic, i.e., it does not involve any image-specific operations. Another interesting avenue for future works would be to assess the effectiveness of FRAug against adversarial attack techniques such as gradient inversion [41, 19]. Finally, it is worth studying the interaction between FRAug and more sophisticated optimization algorithms [6, 25] and communication methods [3, 4].

References

- [1] Mathieu Andreux, Jean Ogier du Terrail, Constance Beguier, and Eric W Tramel. Siloed federated learning for multi-centric histopathology datasets. In *Domain Adaptation and Representation Transfer, and Distributed and Collaborative Learning*, pages 129–139. Springer, 2020.
- [2] Manoj Ghuhan Arivazhagan, Vinay Aggarwal, Aaditya Kumar Singh, and Sunav Choudhary. Federated learning with personalization layers. *arXiv preprint arXiv:1912.00818*, 2019.
- [3] Mingzhe Chen, H Vincent Poor, Walid Saad, and Shuguang Cui. Convergence time optimization for federated learning over wireless networks. *IEEE Transactions on Wireless Communications*, 20(4):2457–2471, 2020.
- [4] Mingzhe Chen, Nir Shlezinger, H Vincent Poor, Yonina C Eldar, and Shuguang Cui. Communication-efficient federated learning. *Proceedings of the National Academy of Sciences*, 118(17), 2021.
- [5] Jia Deng, Wei Dong, Richard Socher, Li-Jia Li, Kai Li, and Li Fei-Fei. Imagenet: A large-scale hierarchical image database. In *2009 IEEE conference on computer vision and pattern recognition*, pages 248–255. Ieee, 2009.
- [6] Yuyang Deng and Mehrdad Mahdavi. Local stochastic gradient descent ascent: Convergence analysis and communication efficiency. In *International Conference on Artificial Intelligence and Statistics*, pages 1387–1395. PMLR, 2021.
- [7] Qi Dou, Daniel Coelho de Castro, Konstantinos Kamnitsas, and Ben Glocker. Domain generalization via model-agnostic learning of semantic features. *Advances in Neural Information Processing Systems*, 32, 2019.
- [8] Alireza Fallah, Aryan Mokhtari, and Asuman Ozdaglar. Personalized federated learning with theoretical guarantees: A model-agnostic meta-learning approach. *Advances in Neural Information Processing Systems*, 33:3557–3568, 2020.
- [9] Yaroslav Ganin and Victor Lempitsky. Unsupervised domain adaptation by backpropagation. In *International conference on machine learning*, pages 1180–1189. PMLR, 2015.
- [10] Xuan Gong, Abhishek Sharma, Srikrishna Karanam, Ziyan Wu, Terrence Chen, David Doermann, and Arun Innanje. Ensemble attention distillation for privacy-preserving federated learning. In *Proceedings of the IEEE/CVF International Conference on Computer Vision*, pages 15076–15086, 2021.
- [11] Xuan Gong, Abhishek Sharma, Srikrishna Karanam, Ziyan Wu, Terrence Chen, David Doermann, and Arun Innanje. Preserving privacy in federated learning with ensemble cross-domain knowledge distillation. 2022.

- [12] Arthur Gretton, Karsten M Borgwardt, Malte J Rasch, Bernhard Schölkopf, and Alexander Smola. A kernel two-sample test. *The Journal of Machine Learning Research*, 13(1):723–773, 2012.
- [13] Weituo Hao, Mostafa El-Khamy, Jungwon Lee, Jianyi Zhang, Kevin J Liang, Changyou Chen, and Lawrence Carin Duke. Towards fair federated learning with zero-shot data augmentation. In *Proceedings of the IEEE/CVF Conference on Computer Vision and Pattern Recognition*, pages 3310–3319, 2021.
- [14] Andrew Hard, Kanishka Rao, Rajiv Mathews, Swaroop Ramaswamy, Françoise Beaufays, Sean Augenstein, Hubert Eichner, Chloé Kiddon, and Daniel Ramage. Federated learning for mobile keyboard prediction. *arXiv preprint arXiv:1811.03604*, 2018.
- [15] Chaoyang He, Murali Annavaram, and Salman Avestimehr. Group knowledge transfer: Federated learning of large cnns at the edge. *Advances in Neural Information Processing Systems*, 33:14068–14080, 2020.
- [16] Kaiming He, Xiangyu Zhang, Shaoqing Ren, and Jian Sun. Deep residual learning for image recognition. In *Proceedings of the IEEE conference on computer vision and pattern recognition*, pages 770–778, 2016.
- [17] Jonathan J. Hull. A database for handwritten text recognition research. *IEEE Transactions on pattern analysis and machine intelligence*, 16(5):550–554, 1994.
- [18] Sergey Ioffe and Christian Szegedy. Batch normalization: Accelerating deep network training by reducing internal covariate shift. In *International conference on machine learning*, pages 448–456. PMLR, 2015.
- [19] Jinwoo Jeon, Kangwook Lee, Sewoong Oh, Jungseul Ok, et al. Gradient inversion with generative image prior. *Advances in Neural Information Processing Systems*, 34:29898–29908, 2021.
- [20] Peter Kairouz, H Brendan McMahan, Brendan Avent, Aurélien Bellet, Mehdi Bennis, Arjun Nitin Bhagoji, Kallista Bonawitz, Zachary Charles, Graham Cormode, Rachel Cummings, et al. Advances and open problems in federated learning. *Foundations and Trends® in Machine Learning*, 14(1–2):1–210, 2021.
- [21] Samuli Laine and Timo Aila. Temporal ensembling for semi-supervised learning. *arXiv preprint arXiv:1610.02242*, 2016.
- [22] Yann LeCun, Léon Bottou, Yoshua Bengio, and Patrick Haffner. Gradient-based learning applied to document recognition. *Proceedings of the IEEE*, 86(11):2278–2324, 1998.
- [23] Da Li, Yongxin Yang, Yi-Zhe Song, and Timothy M Hospedales. Deeper, broader and artier domain generalization. In *Proceedings of the IEEE international conference on computer vision*, pages 5542–5550, 2017.
- [24] Daliang Li and Junpu Wang. Fedmd: Heterogenous federated learning via model distillation. *arXiv preprint arXiv:1910.03581*, 2019.
- [25] Tian Li, Anit Kumar Sahu, Ameet Talwalkar, and Virginia Smith. Federated learning: Challenges, methods, and future directions. *IEEE Signal Processing Magazine*, 37(3):50–60, 2020.
- [26] Tian Li, Anit Kumar Sahu, Manzil Zaheer, Maziar Sanjabi, Ameet Talwalkar, and Virginia Smith. Federated optimization in heterogeneous networks. *Proceedings of Machine Learning and Systems*, 2:429–450, 2020.
- [27] Tian Li, Shengyuan Hu, Ahmad Beirami, and Virginia Smith. Ditto: Fair and robust federated learning through personalization. In *International Conference on Machine Learning*, pages 6357–6368. PMLR, 2021.
- [28] Xiaoxiao Li, Meirui Jiang, Xiaofei Zhang, Michael Kamp, and Qi Dou. Fedbn: Federated learning on non-iid features via local batch normalization. *arXiv preprint arXiv:2102.07623*, 2021.

[29] Tao Lin, Lingjing Kong, Sebastian U Stich, and Martin Jaggi. Ensemble distillation for robust model fusion in federated learning. *Advances in Neural Information Processing Systems*, 33: 2351–2363, 2020.

[30] Quande Liu, Cheng Chen, Jing Qin, Qi Dou, and Pheng-Ann Heng. Feddg: Federated domain generalization on medical image segmentation via episodic learning in continuous frequency space. In *Proceedings of the IEEE/CVF Conference on Computer Vision and Pattern Recognition*, pages 1013–1023, 2021.

[31] Yi Liu, Sahil Garg, Jiangtian Nie, Yang Zhang, Zehui Xiong, Jiawen Kang, and M Shamim Hossain. Deep anomaly detection for time-series data in industrial iot: A communication-efficient on-device federated learning approach. *IEEE Internet of Things Journal*, 8(8):6348–6358, 2020.

[32] Raphael Gontijo Lopes, Stefano Fenu, and Thad Starner. Data-free knowledge distillation for deep neural networks. *arXiv preprint arXiv:1710.07535*, 2017.

[33] Brendan McMahan, Eider Moore, Daniel Ramage, Seth Hampson, and Blaise Aguera y Arcas. Communication-efficient learning of deep networks from decentralized data. In *Artificial intelligence and statistics*, pages 1273–1282. PMLR, 2017.

[34] Yuval Netzer, Tao Wang, Adam Coates, Alessandro Bissacco, Bo Wu, and Andrew Y Ng. Reading digits in natural images with unsupervised feature learning. 2011.

[35] Shiv Shankar, Vihari Piratla, Soumen Chakrabarti, Siddhartha Chaudhuri, Preethi Jyothi, and Sunita Sarawagi. Generalizing across domains via cross-gradient training. *arXiv preprint arXiv:1804.10745*, 2018.

[36] Benyuan Sun, Hongxing Huo, Yi Yang, and Bo Bai. Partialfed: Cross-domain personalized federated learning via partial initialization. *Advances in Neural Information Processing Systems*, 34, 2021.

[37] Canh T Dinh, Nguyen Tran, and Josh Nguyen. Personalized federated learning with moreau envelopes. *Advances in Neural Information Processing Systems*, 33:21394–21405, 2020.

[38] Hemanth Venkateswara, Jose Eusebio, Shayok Chakraborty, and Sethuraman Panchanathan. Deep hashing network for unsupervised domain adaptation. In *Proceedings of the IEEE conference on computer vision and pattern recognition*, pages 5018–5027, 2017.

[39] Garrett Wilson and Diane J Cook. A survey of unsupervised deep domain adaptation. *ACM Transactions on Intelligent Systems and Technology (TIST)*, 11(5):1–46, 2020.

[40] William K Wootters. Statistical distance and hilbert space. *Physical Review D*, 23(2):357, 1981.

[41] Hongxu Yin, Arun Mallya, Arash Vahdat, Jose M Alvarez, Jan Kautz, and Pavlo Molchanov. See through gradients: Image batch recovery via gradinversion. In *Proceedings of the IEEE/CVF Conference on Computer Vision and Pattern Recognition*, pages 16337–16346, 2021.

[42] Lan Zhang and Xiaoyong Yuan. Fedzkt: Zero-shot knowledge transfer towards heterogeneous on-device models in federated learning. *arXiv preprint arXiv:2109.03775*, 2021.

[43] Lin Zhang, Li Shen, Liang Ding, Dacheng Tao, and Ling-Yu Duan. Fine-tuning global model via data-free knowledge distillation for non-iid federated learning. *arXiv preprint arXiv:2203.09249*, 2022.

[44] Yue Zhao, Meng Li, Liangzhen Lai, Naveen Suda, Damon Civin, and Vikas Chandra. Federated learning with non-iid data. *arXiv preprint arXiv:1806.00582*, 2018.

[45] Kaiyang Zhou, Yongxin Yang, Timothy Hospedales, and Tao Xiang. Learning to generate novel domains for domain generalization. In *European conference on computer vision*, pages 561–578. Springer, 2020.

[46] Kaiyang Zhou, Ziwei Liu, Yu Qiao, Tao Xiang, and Chen Change Loy. Domain generalization: A survey. *arXiv e-prints*, pages arXiv–2103, 2021.

- [47] Kaiyang Zhou, Yongxin Yang, Yu Qiao, and Tao Xiang. Domain generalization with mixstyle. *arXiv preprint arXiv:2104.02008*, 2021.
- [48] Zhuangdi Zhu, Junyuan Hong, and Jiayu Zhou. Data-free knowledge distillation for heterogeneous federated learning. In *International Conference on Machine Learning*, pages 12878–12889. PMLR, 2021.